Optical Materials 69 (2017) 339–343

Contents lists available at ScienceDirect

Optical Materials

journal homepage: www.elsevier.com/locate/optmat

Dielectric and structural characterisation of chalcogenide glasses via terahertz time-domain spectroscopy

A. Ravagli [a, *], M. Naftaly [b], C. Craig [a], E. Weatherby [a], D.W. Hewak [a]

[a] Optoelectronics Research Centre, University of Southampton, So17 1BJ, Southampton, UK
[b] National Physical Laboratory, Hampton Road, Teddington, Middlesex, TW11 0LW, UK

ARTICLE INFO

Article history:
Received 20 February 2017
Received in revised form
19 April 2017
Accepted 23 April 2017

Keywords:
Chalcogenide
Glass
Terahertz
Spectroscopy

ABSTRACT

Terahertz time-domain spectroscopy (THz TDS) was used to investigate a series of chalcogenide glasses. In particular, the dielectric properties at terahertz frequencies were determined and correlated with the glass composition. The experimental results showed a strong relationship between the dielectric properties and the polarizability of the glasses studied. A new explanation based on the coordination number of the metallic cations was proposed to understand these observations.

1. Introduction

Chalcogenide glasses are amorphous materials consisting of chalcogen anions and one or more electropositive cations. Chalcogen anions include all the elements of the group XVI of the periodic table. However, the term is generally used only for S, Se and Te, restricting oxide materials to a separate category. The cations commonly used to form chalcogenide glasses belong to the p-block of the periodic table, with some exceptions such as La and Na [1].

The elements forming chalcogenide glasses are generally covalently bonded due to the small difference in electronegativity between cations and anions. As a result, the strength of the bonding is lower than in oxide materials, making glass formation feasible over a large variety of compositions. Indeed, both heteronuclear (e.g., La-S) and homonuclear (Se-Se) bonds can be formed, leading to the formation of non-stoichiometric compounds [1]. Lanthanum and sodium based glasses tend to have a more ionic character due to the weaker electronegativity of these metals [2]. For these glasses, a narrower range of glass-forming composition is found due to the strong tendency to crystallise [3].

The nature of the bonding in chalcogenide glasses gives rise to their unique optical and dielectric properties, such as high refractive index, low phonon energy, photosensitivity and chemical-mechanical durability [1,4,5]. Due to their low phonon energy, chalcogenide glasses are widely employed in infrared optics and photonics for a variety of active and passive applications such as light delivery, supercontinuum generation, fibre lasers, imaging and sensing [6,7].

Previous studies on terahertz properties of glasses were focused on sodosilicate and borosilicate glasses, and on chalcogenide glasses such as GaLaS, AsSe and GeGaSe [8–11]. In this work we report the absorption coefficients and refractive indices in the THz range for 3 compositions of GaLaS glass, for two compositions of the GaLaSSe glass and for 2 compositions of commercial GeSe-based glass, namely IG5 ($Ge_{28}Sb_{12}Se_{60}$) and IG2 ($Ge_{33}As_{12}Se_{55}$). The data was correlated to the mean polarizability of the materials and the impact of charge distribution on the absorption loss was examined. The aim of the study was to develop a deeper understanding of these glassy compounds and to exploit terahertz time-domain spectroscopy (THz TDS) as a useful tool for characterisation of amorphous materials.

2. Experimental

GaLaS and GaLaSSe glasses were prepared using the melt-quenching process as previously reported [12]. Mixtures of La_2S_3, Ga_2S_3 and Ga_2Se_3 were prepared in a dry-nitrogen purged glove-box, avoiding exposure to atmospheric oxygen. The mixtures were

* Corresponding author.
E-mail address: ar1e15@soton.ac.uk (A. Ravagli).

http://dx.doi.org/10.1016/j.optmat.2017.04.057
0925-3467/

homogenised with the aid of a roller mixer for 1 h to enhance the homogenisation of the glasses. Vitreous carbon crucibles were used to contain the precursors during the melting and quenching steps. The crucibles were placed in a silica tube purged with Ar and a split-tube furnace was used to melt the mixtures. The glasses produced by this process were subsequently annealed at 490 °C for 48 h to release internal stresses in the glassy network. Samples for THz measurements were fabricated by cutting the glasses into flats whose faces were lapped and polished to optical finish. Samples of IG2 and IG5 were purchased from Vitron GmbH. The compositions of all glasses are listed in Table 1.

THz optical properties of the glasses were measured by a laboratory-built THz TDS using a standard configuration incorporating a Ti:Sapphire femtosecond laser, four off-axis parabolic mirrors, a biased GaAs emitter, and electro-optic detection with a ZnTe crystal and balanced Si photodiodes [13]. The measurement bandwidth was limited by the dynamic range of the system and sample absorption, and therefore was smaller in more strongly absorbing materials [14].

3. Results and discussion

The absorption coefficients and refractive indices of the investigated chalcogenide glasses are shown in Figs. 1 and 2 respectively, and their values at 0.8 THz are listed in Table 1. The refractive index found for Sample 3 is in good agreement with a previous study which reports a value of ~3.6 at 1 THz [11].

As seen in Table 1, the THz refractive indices of all glasses are much higher than they are in the visible. This is explained by the fact that at THz frequencies the polarizability of polar dielectric materials combines contributions from both electronic and ionic polarizabilities [17]. The electronic component is due to the distortion of the electron charge cloud of the compound by an applied oscillating electric field. Since electrons can respond on short timescales (10^{14}–10^{15} Hz), electronic polarizability operates at frequencies up to the optical regime; this is the mean molecular polarizability quoted in the literature. In contrast, ionic polarizability arises when an applied oscillating field causes vibrational movement of anions and cations with respect to each other, i.e. when it excites optical phonons. Because ionic relaxation times are much slower than electronic, ionic polarizability occurs at lower frequencies; in glasses this is in the THz band. Since ionic polarizability leads to optical phonon excitations, it is also associated with absorption losses.

The relationship between polarizability and refractive index is represented by the Lorentz-Lorenz equation in the form [17–19].

$$\frac{n(f)^2-1}{n(f)^2+2}=\frac{4\pi}{3}Np(f) \quad (1)$$

where $n(f)$ is the frequency-dependent refractive index, $p(f)$ is the frequency-dependent polarizability of the material, and N is the number of molecules per unit of volume. It is important to note that the value of N can vary significantly among different glasses, and can be calculated from the glass composition using the formula [18].

$$N=\frac{\rho}{MW}N_A \quad (2)$$

where ρ is the density of the material in $g\cdot m^{-3}$, MW is the molecular weight of the composition in $g\cdot mol^{-1}$ and N_A is the Avogadro's number. The difference between the refractive indices of a material at THz and optical frequencies therefore represents the contribution of its ionic polarizability.

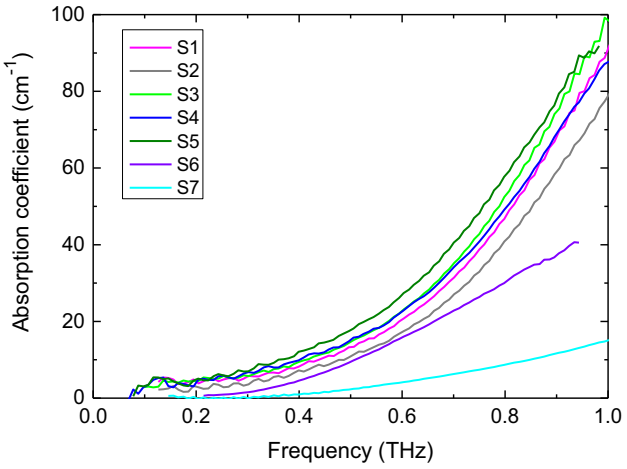

Fig. 1. Absorption coefficients of the glasses studied.

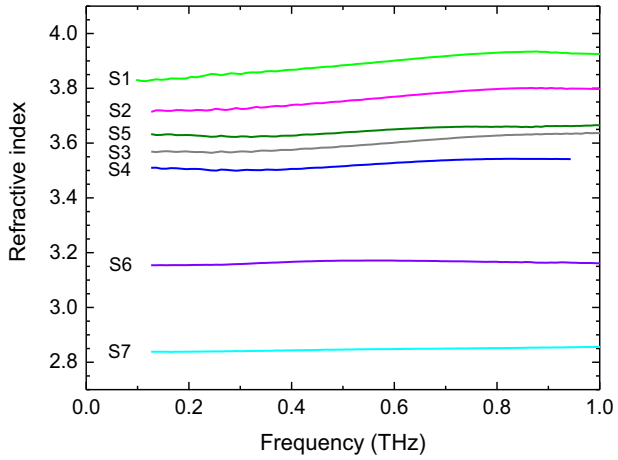

Fig. 2. Refractive indices of the glasses studied.

Table 1
Composition of the investigated glasses and their density, optical refractive index, and refractive index and absorption coefficient at 0.8 THz.

Sample number	Composition	Density (g/cm)	Optical refractive index @ 1.5 μm	Refractive index @ 0.8 THz	Absorption coefficient @ 0.8 THz (cm^{-1})
1	$La_{20}Ga_{20}S_{60}$	4.27	2.37 ± 0.04[a]	3.93 ± 0.01	52 ± 2
2	$La_{16}Ga_{24}S_{60}$	4.48	2.38 ± 0.04[a]	3.80 ± 0.01	46 ± 2
3	$La_{12}Ga_{28}S_{60}$	4.11	2.37 ± 0.04[a]	3.63 ± 0.01	40 ± 2
4	$La_{12}Ga_{28}S_{48}Se_{12}$	3.99	2.31 ± 0.04 [12]	3.54 ± 0.01	51 ± 2
5	$La_{12}Ga_{28}S_{39}Se_{21}$	4.21	2.37 ± 0.04 [12]	3.66 ± 0.01	60 ± 3
6	$Ge_{28}Sb_{12}Se_{60}$ (IG5)	4.41	2.60 [15]	3.17 ± 0.01	31 ± 1
7	$Ge_{33}As_{12}Se_{55}$ (IG2)	4.66	2.73 [16]	2.85 ± 0.01	9 ± 0.5

[a] Measured using ellipsometry.

The polarizability of the glasses studied has been calculated from Eqs. (1) & (2) and is listed in Table 2 together with the mean atomic polarizability from literature. It is seen that for the GLS glass series (samples 1–5) the total polarizability (calculated from Eqs. (1) and (2)) was larger than the mean atomic value by a factor of about 3; whereas for the GeSe-based glasses (samples 6 & 7) the difference was very small. This indicates that glasses 6 & 7 have low ionic polarizability. As a result, they also have much lower absorption coefficients (Fig. 1 & Table 1), as well as lower THz refractive indices; whereas their optical refractive indices are higher than in GLS glasses.

The high ionic polarizability of GLS and GLSSe glasses may be attributed to the presence of La. Previous studies have shown that La^{3+} can coordinate a large number of atoms, as many as 6–7 [20,21]. This results in a complex glassy network with many reconfigurable bonds, which are therefore highly polarizable.

Since, as explained above, at THz frequencies both refractive index and absorption coefficient increase with ionic polarizability, it is of interest to consider the relationship between them, as presented in Fig. 3. It is seen that the examined glasses fall into two groups, each having a roughly linear relationship between absorption and refractive index, but with different slopes. One group has glasses containing Se, whilst the other has pure GLS glasses containing only S. The addition of Se increases the polarizability, because Se is larger than S, with weaker bonds that are more polarizable. Moreover, the presence of both Se and S increases charge disorder; as explained below, this causes increased absorption. Therefore the series of glasses containing S + Se lie on a steeper absorption slope than those containing only S. It is also seen that both absorption and refractive index increase with the presence of La^{3+}, because as mentioned above it increases the complexity of the glass network, causing both higher polarizability and larger charge disorder.

The frequency dependence of far-infrared absorption in amorphous materials has been analysed in terms of disorder-induced coupling of radiation into the optical phonon modes [22], with the frequency dependence of absorption being described by the power law relation

$$n(f)\alpha(f) = Kf^{\beta} \tag{3}$$

where $\alpha(f)$ is the frequency-dependent absorption coefficient, and K and β are material-dependent parameters. The coefficient K increases proportionately with the density of charge fluctuations, and therefore is related to disorder in the glass structure; multicomponent glasses tend to have larger values of K [9,18]. The exponent β is expected to be ~2 for glasses [22]; indeed an alternative model assumes a square law relationship [23]. However, the fit to the square law was found to be very poor, as illustrated for Sample 3 in Fig. 4.

The data for all glasses was fitted to Eq. (3) and the fitting parameters are summarised in Table 2. It is seen that the value of K is higher for materials with higher polarizability. This is consistent with the fact that materials with large charge disorder tend to be more strongly polarizable. It is of interest to consider the relationships between K and n, and between β and n, as shown in Fig. 5. As may be expected, the correlation between K and n (Fig. 5a) is similar in character to that between α and n (Fig. 4), since K is roughly proportional to absorption (for similar values of n and β). Charge disorder is determined by the chemical composition of the samples. As discussed above, the concentration of La in the glass affects its charge spatial disorder, due to its large coordination ability which results in a dramatic growth in the number of possible spatial arrangements in the glassy network (K increases from sample 1 to 2 to 3). On the other hand, in the case of GLSSe glasses, the formation of Se-O and O-Se-O, due to the presence of oxygen impurities, can change the oxidation state of Se from 2- to 2+, thus also increasing the charge disorder (K is larger in sample 5 than in sample 4).

Table 2
Mean molecular polarizability of the glasses studied; their total polarizability at 0.8 THz calculated from Eqs. (1) and (2); and the fitting parameters to the absorption Eq. (3) $n\alpha = Kf^{\beta}$ for amorphous materials.

Sample number	Mean molecular polarizability from literature (atomic units)	Reference	Total polarizability @ 0.8 THz from Eqs. (1) and (2) (atomic units)	K (cm^{-1})	β
1	64.74	[23–25]	158 ± 8	380 ± 1	3.08 ± 0.02
2	58.53	[23–25]	142 ± 7	339 ± 1	3.25 ± 0.02
3	52.33	[23–25]	144 ± 7	280 ± 1	3.09 ± 0.03
4	53.12	[23–25]	154 ± 8	315 ± 1	3.05 ± 0.02
5	53.72	[23–25]	163 ± 8	359 ± 2	2.73 ± 0.03
6	32.6	[23,26,27]	36 ± 2	161 ± 1	1.91 ± 0.04
7	31.32	[23,26,27]	35 ± 2	43.6 ± 0.3	2.66 ± 0.02

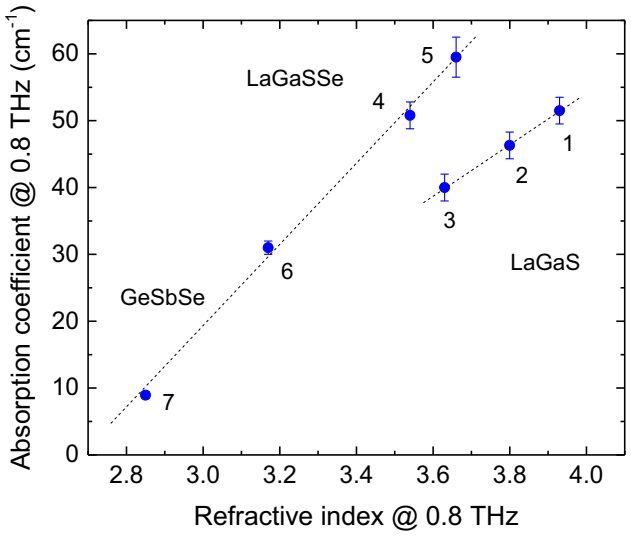

Fig. 3. Correlation between the absorption coefficient and refractive index at 0.8 THz. Numbers denote sample numbers.

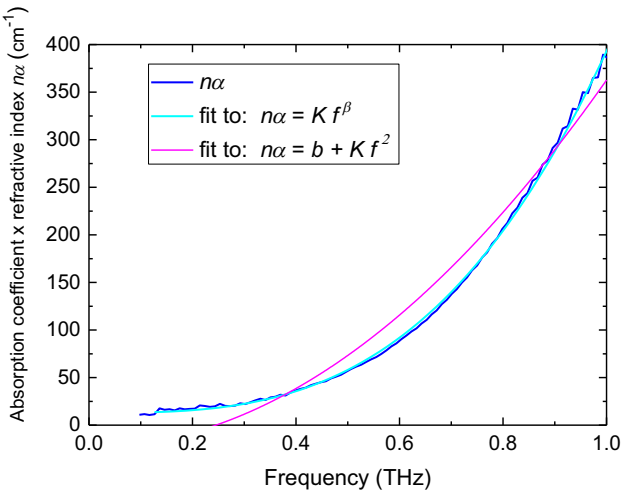

Fig. 4. Least-squares fit of the product $n\alpha$ to Eq. (3) and to the square law, demonstrating that Eq. (3) is a better fit.

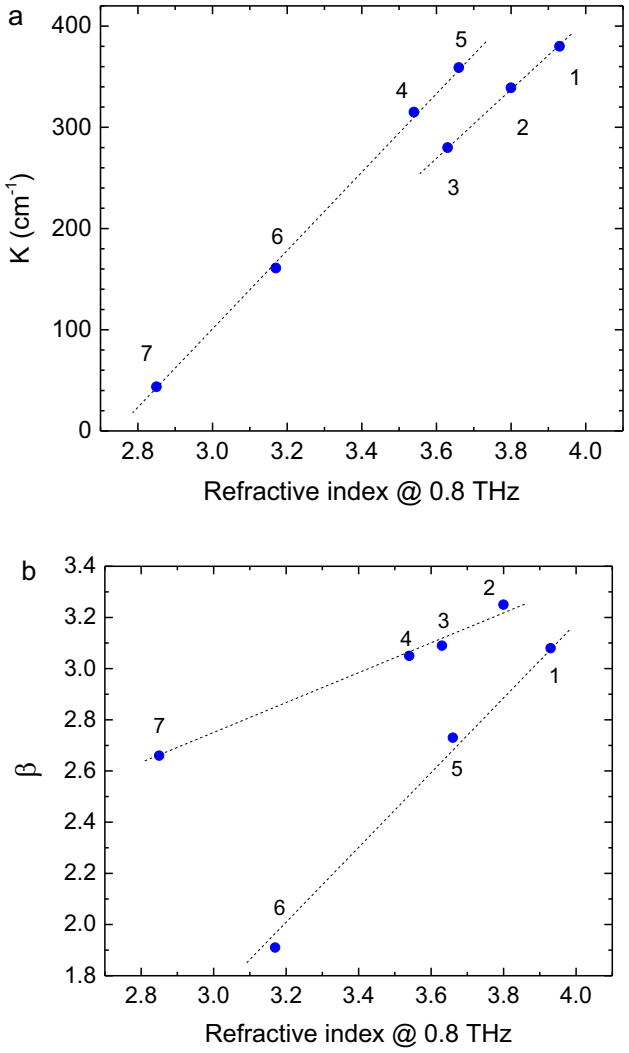

Fig. 5. a) Relationship between K and refractive index at 0.8 THz. b) Relationship between β and refractive index at 0.8 THz. Numbers denote sample numbers.

Table 3
Value of β reported for glasses.

Composition	β	Reference
$La_{12}Ga_{28}S_{60}$	3.09	This work
$La_{16}Ga_{24}S_{60}$	3.25	This work
$La_{20}Ga_{20}S_{60}$	3.08	This work
$La_{12}Ga_{28}S_{48}Se_{12}$	3.05	This work
$La_{12}Ga_{28}S_{39}Se_{21}$	2.73	This work
$Ge_{28}Sb_{12}Se_{60}$ (IG5)	1.91	This work
$Ge_{33}As_{12}Se_{55}$ (IG2)	2.66	This work
$As_{40}S_{60}$	1.95	[21,27]
$As_{40}Se_{60}$	2.0	[21]
$Ge_{30}As_8Ga_2Se_{60}$	2.0	[10]
$Ge_{35}Ga_5Se_{60}$	2.0	[10]
$Ge_{10}As_{20}S_{70}$	2.0	[10]
$Tl_2SeAs_2Te_3$	1.9	[21]
Quartz	2.0	[9]
Amorphous silica SiO_2	2.0	[8,21]
GeO_2	2.0	[21]
B_2O_3	2.0	[21]
Pyrex	1.97	[9]
BK7	2.28	[9]
SK10	2.80	[9]

The relationship between β and n (Fig. 5b) is puzzling, and may be related to the degree of disorder on various scales of the glass network, since β reflects the amorphicity of the structure. Table 3 compares the value of the exponent β reported in different glasses. However, in several of these, $\beta = 2$ was assumed rather than used as a fitting parameter [9,22]. Many of the glassy materials reported in literature (e.g. silica, quartz, GeGaAsSe, pyrex) contain mainly 4-fold coordinated cations, which appear to give rise to a β~2 behaviour. On the other hand, a previous study reported a value of $\beta = 2.3$ for the BK7 glass containing 9mol% sodium [8] and $\beta = 2.8$ for SK10 glass containing 48mol% BaO and 12mol% B_2O_3 [8], leading to suppose that $\beta > 2$ for glasses with high coordination numbers. Sodium and lanthanum are both capable of bonding a large number of anions around their coordination shells. In particular, sodium was reported to coordinate up to 8 chalcogenide anions and lanthanum up to 7 [20,21]. The values of β in GLS and GLSSe glasses are found to be as high as 3, supporting the hypothesis of a relationship between β and the coordination number. Since, as discussed above, high coordination number also tends to increase polarizability, higher values of β should be correlated with higher refractive indices, as seen in Fig. 5b.

4. Conclusions

The THz optical properties of a variety of chalcogenide glasses have been investigated using time-domain spectroscopy. The refractive indices and absorption coefficients of seven samples of GLS, GLSSe, and GaSe-based glasses were obtained in the range between 0.3 THz and 1 THz. The results were found to be strongly correlated with glass composition, specifically with the content of La and Se. The refractive indices were analysed in relation to electronic and ionic polarizabilities of the glass. The absorption coefficients were fitted to the power-law function, where the variation of the coefficient with glass composition could be explained in terms charge disorder. It is speculated that the unusually high values of the power exponent (β~3) may be attributed to the large coordination number of La. Further studies may confirm whether the value of the exponent β can be employed for structural studies of amorphous materials. Although further investigations are required, these results demonstrate the usefulness of THz spectroscopy as a tool in the study of glasses.

Acknowledgements

This work is funded by the UK Engineering and Physical Sciences Research Council (EPSRC) grant EP/M015130/1 for ChAMP, the Chalcogenide Advanced Manufacturing Programme. We have no underpinning data that needed archival storage within the content of this work.

References

[1] A.B. Seddon, Chalcogenide glasses: a review of their preparation, properties and applications, J. Non. Cryst. Solids 184 (1995) 44–50, http://dx.doi.org/10.1016/0022-3093(94)00686-5.
[2] D. Lide, CRC Handbook of Chemistry and Physics, 84th, Memory, 2003, http://www.mendeley.com/research/crc-handbook-chemistry-physics-84th/.
[3] J.D. Shephard, R.I. Kangley, R.J. Hand, D. Furniss, C.A. Miller, A.B. Seddon, Properties of Ga-La-Na sulphide glasses, J. Non. Cryst. Solids 332 (2003) 271–278, http://dx.doi.org/10.1016/j.jnoncrysol.2003.07.002.
[4] A. Zakery, S. Elliott, Optical properties and applications of chalcogenide glasses: a review, J. Non. Cryst. Solids 330 (2003) 1–12, http://dx.doi.org/10.1016/j.jnoncrysol.2003.08.064.
[5] B.J. Eggleton, B. Luther-Davies, R. Kathleen, Chalcogenide photonics, Nat. Photonics 5 (2011) 725, http://dx.doi.org/10.1038/nphoton.2011.309.
[6] I.D. Aggarwal, J.S. Sanghera, Development and applications of chalcogenide glass optical, J. Optoelectron. Adv. Mater 4 (2002) 665–678, http://dx.doi.org/10.1080/01468030050058811.
[7] I.D. Aggarwal, J.S. Sanghera, Development and applications of chalcogenide

glass optical fibers at NRL, J. Optoelectron. Adv. Mater. 4 (2002) 665–678. http://joam.inoe.ro/arhiva/pdf4_3/Aggarwal.pdf.
[8] E.P.J. Parrott, J.A. Zeitler, G. Simon, B. Hehlen, L.F. Gladden, S.N. Taraskin, S.R. Elliott, Atomic charge distribution in sodosilicate glasses from terahertz time-domain spectroscopy, Phys. Rev. B - Condens. Matter Mater. Phys. 82 (2010), http://dx.doi.org/10.1103/PhysRevB.82.140203.
[9] M. Naftaly, R.E. Miles, Terahertz time-domain spectroscopy of silicate glasses and the relationship to material properties, J. Appl. Phys. 102 (2007), http://dx.doi.org/10.1063/1.2771049.
[10] S.B. Kang, M.H. Kwak, B.J. Park, S. Kim, H.C. Ryu, D.C. Chung, S.Y. Jeong, D.W. Kang, S.K. Choi, M.C. Paek, E.J. Cha, K.Y. Kang, Optical and dielectric properties of chalcogenide glasses at terahertz frequencies, ETRI J. 31 (2009) 667–674, http://dx.doi.org/10.4218/etrij.09.1209.0028.
[11] M. Zalkovskij, C. Zoffmann Bisgaard, A. Novitsky, R. Malureanu, D. Savastru, A. Popescu, P. Uhd Jepsen, A.V. Lavrinenko, Ultrabroadband terahertz spectroscopy of chalcogenide glasses, Appl. Phys. Lett. 100 (2012), http://dx.doi.org/10.1063/1.3676443.
[12] A. Ravagli, C. Craig, J. Lincoln, D. Hewak, Ga-La-S-Se glass for visible and thermal imaging, Adv. Opt. Mater. (n.d.).
[13] M. Naftaly, R. Dudley, Linearity calibration of amplitude and power measurements in terahertz systems and detectors, Opt. Lett. 34 (2009) 674–676, http://dx.doi.org/10.1364/OL.34.000674.
[14] P. Jepsen, B. Fischer, Dynamic range in terahertz time-domain transmission and reflection spectroscopy, Opt. Lett. 30 (2005) 29, http://dx.doi.org/10.1364/OL.30.000029.
[15] IG5 (Ge28Sb12Se60), (n.d.). http://www.vitron.de/datasheets/VITRON IG-5 Datenblatt Jan 2015.pdf.
[16] IG2 (Ge33As12Se55), (n.d.). http://www.vitron.de/datasheets/VITRON IG-2 Datenblatt Jan 2015.pdf.
[17] J.A. Duffy, Bonding, Energy Levels and Bands in Inorganic Solids, Longman Scientific & technicals, New York [NY], 1990.
[18] C.Z. Tan, J. Arndt, The mean polarizability and density of glasses, Phys. B Condens. Matter. 229 (1997) 217–224, http://dx.doi.org/10.1016/S0921-4526(96)01032-0.
[19] A. Choudhury, P.K. Dorhout, Synthesis, structure, and optical properties of the quaternary seleno-gallates NaLnGa 4 Se 8 (Ln, La, Ce, Nd) and their comparison with the isostructural thio-gallates, Inorg. Chem. 47 (2008) 3603–3609.
[20] R. Li, A.B. Seddon, Gallium-lanthanum-sulphide glasses: a review of recent crystallisation studies, J. Non. Cryst. Solids 257 (1999) 17–24, http://dx.doi.org/10.1016/S0022-3093(99)00485-8.
[21] U. Strom, P.C. Taylor, Temperature and frequency dependences of the far-infrared and microwave optical absorption in amorphous materials, Phys. Rev. B 16 (1977) 5512.
[22] S.N. Taraskin, S.I. Simdyankin, S.R. Elliott, J.R. Neilson, T. Lo, Universal features of terahertz absorption in disordered materials, Phys. Rev. Lett. 97 (2006), http://dx.doi.org/10.1103/PhysRevLett.97.055504.
[23] E.A. Reinsch, W. Meyer, Finite perturbation calculation for the static dipole polarizabilities of the atoms Na through Ca, Phys. Rev. A 14 (1976) 915–918, http://dx.doi.org/10.1103/PhysRevA.14.915.
[24] R. Alpher, D. White, Optical refractivity of high-temperature gases. I. Effects resulting from dissociation of diatomic gases, Phys. Fluids (1959) 153–161, http://dx.doi.org/10.1063/1.1705906, 1. 2.
[25] B.O. Roos, R. Lindh, P.Å. Malmqvist, V. Veryazov, P.O. Widmark, Main group atoms and dimers studied with a new relativistic ANO basis set, J. Phys. Chem. A 108 (2004) 2851–2858, http://dx.doi.org/10.1021/jp031064+.
[26] C. Thierfelder, B. Assadollahzadeh, P. Schwerdtfeger, S. Schäfer, R. Schäfer, Relativistic and electron correlation effects in static dipole polarizabilities for the group-14 elements from carbon to element Z=114: theory and experiment, Phys. Rev. A - At. Mol. Opt. Phys. 78 (2008) 1–7, http://dx.doi.org/10.1103/PhysRevA.78.052506.
[27] S. Onari, K. Matsuishi, T. Arai, Far-infrared absorption spectra and the spatial fluctuation of charges on amorphous As-S and As-Se systems, J. Non Cryst. Solids 86 (1986) 22–32.